

**A Phenomenological Study of
Interlayer Tunneling in Double-Layered
Quantum Hall Systems**

X. G. WEN¹ & A. ZEE²

¹ *Department of Physics
Massachusetts Institute of Technology
77 Massachusetts Avenue
Cambridge, MA 02139, USA*

² *Institute for Theoretical Physics
University of California
Santa Barbara, CA 93106, USA*

ABSTRACT: We study interlayer transport in double-layered (*mmm*) quantum Hall liquids in the weak tunneling limit, in particular the effects of lead geometry on the I-V characteristics of interlayer tunneling. We proposed several practical ways to study experimentally the novel interlayer transport properties in the double-layered (*mmm*) quantum Hall liquids. Some concrete predictions on the DC characteristics, narrow band noises, and finite temperature effects are given. We also clarify certain issues related to interlayer tunneling. In particular we discuss the similarities and differences between interlayer transports in Hall fluids and Josephson tunneling in superconductors.

I. INTRODUCTION

In a work^{1,2}, we pointed out that certain multilayer quantum Hall states (in the absence of interlayer tunneling) have superfluidity/superconductivity as a result of spontaneous broken $U(1)$ symmetry, which leads to novel interlayer transport properties. This special type of quantum Hall states may manifest itself in various experimental situations. In particular, one such quantum Hall liquid is a double layered quantum Hall state with topological order described by the matrix

$$K = \begin{pmatrix} m & m \\ m & m \end{pmatrix} \quad (1)$$

(*i.e.*, the (mmm) state.) This state has a filling factor $\nu = 1/m$ and contains a low lying collective mode.^{3,1} The interlayer tunneling current in such a state behave in a way reminiscent of Josephson tunneling between superconducting thin films. Recent experiment⁴ confirmed the predicted similarity between the interlayer tunneling in (111) quantum Hall state and the tunneling between two superconducting thin films.

In our work we emphasized the many significant distinctions as well as similarities between the effects we discussed and the Josephson effects, so that to avoid confusion, it may be best not to refer to the effects discussed in Ref. 1,2 as Josephson effects. There has been some interesting discussion on some of the distinctions between the two effects.⁵ One purpose of this paper is to add to this discussion, and we hope to clarify some of these distinctions and similarities.

Another purpose of this paper is to add to our previous work by studying the various different ways in which leads can be attached to the double layered system. The resulting interlayer tunneling currents in these different situations have different spatial distributions. Thus, different arrangements may lead to different experimental consequences, due to the non-zero Hall conductance σ_{xy} in the (mmm) state.

We may also emphasize here that we always worked in the limit of small interlayer tunneling amplitude. As the tunneling amplitude becomes large, with electrons moving relatively freely between the two layers, we have effectively a single layered system and, strictly speaking, should no longer think of a double layered system. However, we show in this paper that all the experimental predictions obtained in the weak tunneling limits do cross over to the expected results of a single layered system in the strong tunneling limits.

This paper contains several sections which use quite different methods to address the interlayer transport from different angles and limits. Thus it may be helpful to summarize the motivations and the results in each section here.

In section 2 we give a brief review of the results and formalism developed in Ref. 1,2 for the double layer (*mmm*) state. The purpose of the review is to setup the stage for discussions in the later sections. We also discussed the DC interlayer tunneling, assuming the two leads are uniformly attached to the two layers of the (*mmm*) state. We show that for this lead-geometry, the voltage drop between the two layers vanishes if the tunneling current is less than a critical value

$$I_c \sim \frac{1}{2} e N_e \frac{\Delta_{SAS}}{\hbar} \quad (2)$$

where N_e is the total number of electrons and Δ_{SAS} is the energy splitting between the states with wave functions symmetric and antisymmetric between the two layers⁶. The value of I_c will be drastically reduced if the magnetic field has a component parallel to the layers.

The lead geometry assumed in section 2 is not practical. Thus in section 3 we study a more realistic lead-geometry where one lead is attached to one point in the first layer and the other lead is attached to a different point in the second layer. In this case, the components of the current parallel to the layer will no longer vanish. This will reduce the critical tunneling current I_c and, due to the finite Hall conductance, cause a finite and

quantized conductance $I/V = \frac{e^2}{mh}$ if the tunneling current is less than the critical value. The coherent tunneling between the two layers is reflected by the fact that the tunneling conductance is finite $\sigma = \frac{e^2}{mh}$ no matter how weak is the interlayer tunneling amplitude. A weak interlayer tunneling amplitude only reduces the critical tunneling current I_c . For the point-contact leads, we find, for small systems, I_c is given by (2); while for large systems, it crosses over to

$$I_c \sim \left(\frac{f_v^2}{\epsilon}\right) \frac{1}{\ln(l/l_0)} \frac{e^2}{d\hbar} e = \left(\frac{f_v^2}{\epsilon}\right) \frac{1}{\ln(l/l_0)} \frac{100\text{\AA}}{d} 35\mu\text{A}$$

where l is a characteristic length scale and f_v is a dimensionless function of d/l_B (the ratio between the interlayer separation d and the magnetic length l_B). Very roughly $I_c \sim 100\text{nA}$ or less (due to the parallel magnetic field). Notice that for point-contact lead the critical tunneling current is not proportional to the area of the sample.

In section 4 and section 8 we study the narrow band noise and AC effects in interlayer tunneling. We show that, in the weak tunneling limit and below the critical tunneling current, the tunneling current contains a narrow band noise centered at the frequency $f_0 = eV/h$ which is one-half of the usual Josephson frequency $2eV/h$. However, we still lack of a reliable calculation of the band width. The discussions in section 8 suggest that the width of the peak can be less than Δ , the energy gap of the neutral collective mode induced by interlayer tunneling.

The section 5 covers the effect of the interlayer tunneling (with point and surface tunneling junction) on the dynamics of the collective modes. The discussions there apply to both double-layered (mmm) state and usual superconductor. We find that the tunnelings in both systems are described by the same equation. This suggests that tunnelings in the two systems demonstrate the same phenomena. The discussions are also motivated by a concern that the changes in the dynamics of the collective modes caused by the tunneling may affect the Josephson effect in the usual superconductors, and the narrow band noise

in the double-layered system. For example the surface junction between the two layers open up an energy gap Δ for the superfluid mode. This energy gap may affect the width of the narrow band noise. However, from the discussions in section 5, we find that the point junction do not change the dynamics of the collective mode, and the narrow band noise in the tunneling current through a point junction may have nearly zero band width.

The section 6 addresses the relationship between the easy plane ferromagnets and the XY model. An easy plane ferromagnet is closely related to the double layer (mmm) state, and the XY model to the ordinary superconductor. We find that the two models have identical equations of motion (after renaming some parameters) at low energies and in the weak tunneling limit. This establishes the close relationship between the double-layered (mmm) state and two dimensional superfluid.

In section 7 we propose a four terminal measurement which allow us to test the prediction that a small interlayer tunneling current does not induce any voltage drop between the two layers for the (mmm) state.

In section 9 we perform a perturbative calculation of interlayer transport at finite temperatures in weak interlayer tunneling amplitude limit. We find that, at the leading order of the interlayer tunneling amplitude, $I \propto V^\gamma$ at finite temperatures. The temperature dependent exponent satisfies $\gamma \rightarrow 0$ as $T \rightarrow 0$ and $\gamma \rightarrow 1/4$ as T approaches the K-T transition temperature T_{KT} . The differential conductance at $V = 0$ is infinite for $T < T_{KT}$. Again we see that the interlayer tunneling is drastically enhanced in the (mmm) state. The noise spectrum $F(\omega)$ is found to have an algebraic singularity at $\omega = eV/\hbar$. If the tunneling only occurs at isolated points, we have $F(\omega) \sim |eV/\hbar - \omega|^{\gamma-1}$. The algebraic properties at finite temperatures are due to the algebraic long range order in the order parameter.

In summary we see that the double-layered (mmm) state demonstrates a lot of similar properties of two dimensional superfluid. It would be very interesting to fabricate samples

with very weak interlayer tunneling amplitude to study the superfluid mode in the (mmm) state.

II. DC INTERLAYER TUNNELING – A BRIEF REVIEW

Let us sketch briefly the discussion in Ref. 1,2 to which the reader is referred for details. In a series of papers⁷ we have developed a simple and unified classification of abelian fractional quantum Hall states, based on Chern-Simons effective theory. The topological order inherent in these states are characterized by a κ -by- κ matrix we call K .⁸ The corresponding low energy effective field theory contains κ gauge potentials a_μ , whose masses are proportional to the eigenvalues of K . We start by asking what happens when one of these eigenvalues vanishes, for example, for the matrix in (1). There is now evidence that a quantum Hall state characterized by this matrix (known as the (mmm) state) has been observed experimentally⁹ for $m = 1$ in double layered systems. Since K has one zero eigenvalue in the (mmm) state, one of the gauge potentials is massless, corresponding to a gapless linearly dispersing mode. Conceptually, this may be associated with the appearance of an off-diagonal long range order associated with a spontaneously broken $U(1)$ symmetry with $\langle c_1^\dagger c_2 \rangle \propto e^{i\theta}$, where c_1 and c_2 denote the electron annihilation operator in layer 1 and 2 respectively. The fluctuations of this angle field give rise to a gapless mode described by the Lagrangian

$$\mathcal{L} = \frac{c}{2}((\partial_t \theta)^2 - v^2(\partial_i \theta)^2) \quad (3)$$

Here c may be thought of as the capacitance per unit area between the two layers. The effective capacitance of the system is given by $C = cA$ with A the area of the double layered Hall system. In this paper we will choose units in which $e^2 = \hbar = 1$ unless explicitly stated otherwise.

When interlayer tunneling is “switched” on, this $U(1)$ symmetry is explicitly broken. In our Chern-Simons theory description of the double-layered FQH liquids, the interlayer tunneling is described by a plasma of magnetic monopoles and anti-monopoles. An angular order parameter field $\theta(x, t)$ is introduced to couple to the density of monopoles. In the limit of weak tunneling amplitude, corresponding to a dilute density of monopoles, we can derive the effective Lagrangian

$$\mathcal{L} = \frac{c}{2}((\partial_t\theta)^2 - v^2(\partial_i\theta)^2) + \eta \cos \theta \quad (4)$$

with η proportional to the tunneling amplitude. In terms of Δ_{SAS} (the energy splitting between the states with wave functions symmetric and antisymmetric between the two layers⁶) the tunneling coefficient η is given by

$$\eta = \frac{1}{2}n\Delta_{SAS} \quad (5)$$

where n is the total density of electrons in the two layers.

Various physical quantities can be expressed in terms of the θ field. The difference in electron density $n_- = n_1 - n_2$ and the difference in electron current density j_- between the two layers are given by

$$n_- = 2c\partial_t\theta, \quad j_{-,i} = 2v^2c\partial_i\theta \quad (6)$$

The tunneling current density between the two layers is given by

$$j_t = \eta \sin \theta \quad (7)$$

We recognize that the equation of motion from the Lagrangian (4)

$$c(\partial_t^2 - v^2\partial_i^2)\theta + \eta \sin \theta = 0 \quad (8)$$

is nothing other than the conservation of electrons

$$\partial_t n_- - \partial_i j_{-,i} + 2j_t = 0 \quad (9)$$

The voltage difference between the two layers is (see Ref. 2 and section VI below)

$$V = \frac{\hbar \partial_t \theta}{e} \quad (10)$$

When leads are attached, electrons can flow in and out of the system and the right hand side of (9) is no longer zero. Within the semiclassical approximation (*i.e.*, treating θ as a classical field), the tunneling I-V characteristics can be easily obtained from the equations above. Let us attach two leads to the first and the second layer and connect the two leads to a voltage source through a resistor R_{ex} . The current injected from the lead is given by

$$I = R_{ex}^{-1}(V_{ex} - V) \quad (11)$$

where V_{ex} is the external voltage. (See Fig. 1) This current is diminished by incoherent tunneling. Let A denote the area of the sample and R_{leak} the leak resistance due to incoherent tunneling between the two layers. Then, upon integrating (9) over the area and assuming θ and η to be independent of \vec{x} , we determine the change in the difference in the number of electrons in the two layers $N_- = \int d^2x n_-$ to be given by

$$\frac{1}{2} \frac{dN_-}{dt} + A\eta \sin \theta = \frac{V_{ex} - V}{eR_{ex}} - \frac{V}{eR_{leak}} \quad (12)$$

We may rewrite (12) as

$$Ac \frac{d^2 \theta}{dt^2} = -A\eta \sin \theta + R_{ex}^{-1} \left(\frac{1}{e} V_{ex} - \frac{\hbar}{e^2} \frac{d\theta}{dt} \right) - \frac{\hbar}{e^2} R_{leak}^{-1} \frac{d\theta}{dt} \quad (13)$$

For isolated and dissipationless system ($R_{ex} = \infty$ and $R_{leak} = \infty$), (13) reduces to (8) (with space independent θ .)

Our confidence in this equation is bolstered by the fact that it can be derived from general principles as shown in Ref. 2. Furthermore, it is worth emphasizing that this equation has the same structure as a simple circuit diagram equation from “high school physics.” Consider the circuit diagram indicated in Fig. 1 where for the moment we do

not specify what the black box contains. The current going through R_{ex} is given by $I = (V_{ex} - V)/R_{ex}$ where V is just the voltage across the black box as indicated in the diagram and may be measured by an experimenter. By current conservation, the current I_{bb} going through the black box is given by

$$I_{bb} = R_{ex}^{-1}(V_{ex} - V) - R_{leak}^{-1}V \quad (14)$$

We are to solve for V and hence determine I . This procedure holds regardless of what the black box might contain, of course, but to solve the equation we must be told how I_{bb} is related to V , namely the $I - V$ characteristics of the black box. For example, suppose the black box contains a resistor of resistance R_{bb} . Then $I_{bb} = V/R_{bb}$. Now V and I can be determined. Here we are saying that if the black box contains a double layered quantum Hall junction with the $I - V$ characteristics

$$I_{bb} = eAc \frac{dV}{dt} + eA\eta \sin(\theta_0 + \int_0^t dt' V(t')) \quad (15)$$

This when combined with (14) and (10) is just (13).

We observe that these equations manifestly have a time independent solution given by

$$V = 0 \quad (16)$$

and

$$I = I_{bb} = V_{ex}/R_{ex} \quad (17)$$

Since I_{bb} is also equal to $eA\eta \sin \theta_0$, we see that the maximum current I_c is given by $I_c = A\eta$ (See Fig. 2a).

In this solution the voltage drop V across the two layers is zero and thus the current is dissipationless. Notice that no matter how small is the interlayer tunneling strength η the voltage V remains zero as long as the current is less than I_c . A weak tunneling amplitude only reduces I_c , the range of current over which the voltage drop vanishes. Notice also that in this solution no current flows through the resistor R_{leak} .

III. LEAD GEOMETRY – POINT LEADS

In the above calculation we have assumed that the external leads are ideal and draws current uniformly across the area of the two layers. In other words, the leads are treated as theoretical leads with “area contact.” The current flows from one layer to the other without current flowing in the directions parallel to the plane (*i.e.*, in the x and y directions). In practice, leads may have point-like contacts, and in general, are attached to different points of the sample, in which case the x - y components of the current will no longer vanish and we cannot assume $\partial_i\theta = 0$. The current in the x - y directions has another important effect. Due to the Hall conductance σ_{xy} this in-plane current would induce a voltage drop in the x - y directions. Thus the voltage difference between the two leads is not only the relative voltage between the two layers, but also receives a contribution from the voltage drop in the x - y directions.

To be specific let us consider a rectangular sample of length L and width W in Fig. 3, with boundaries at $x = \pm\frac{L}{2}$ and at $y = \pm\frac{W}{2}$. A lead is attached the first layer at point $(x, y) = (\frac{L}{2}, 0)$ and another lead is attached to the second layer at $(x, y) = (-\frac{L}{2}, 0)$. We would like to determine the two-terminal I-V characteristics for this lead geometry.

We draw two small (semi-circular say, if one wishes to be definite) areas around $(\frac{L}{2}, 0)$ and $(-\frac{L}{2}, 0)$ of radius a . Outside these two small areas the equation of motion for θ takes the form

$$c[\frac{d^2\theta}{dt^2} - v^2\partial_i^2\theta] = -\eta \sin\theta - r_{leak}^{-1} \frac{d\theta}{dt} \quad (18)$$

where r_{leak}^{-1} is the leak conductance per unit area. The boundary condition for θ is that $\vec{n}_\perp \cdot \vec{\partial}\theta = 0$ except around the leads at $(x, y) = (\pm\frac{L}{2}, 0)$. (Here \vec{n}_\perp is the vector perpendicular to the boundary.)

Around $(x, y) = (\pm \frac{L}{2}, 0)$ we have the condition (from (12)) that

$$\frac{dN_-}{dt} = \frac{V_{ex} - V_{AB}}{eR_{ex}} = \int d^2x \partial_i j_{-,i} = \int dl_i j_{-,i}, \quad (19)$$

where the integration is over and around the small areas carved out around the leads. The interlayer voltage V in (12) is replaced by $V_{AB} = V_A - V_B$ where V_A is the voltage in the first layer at the point $(x, y) = (\frac{L}{2}, 0)$ and V_B is the voltage in the second layer at the point $(x, y) = (-\frac{L}{2}, 0)$. (Note the interlayer voltage V is defined as the voltage difference between the two layers at the *same* point in the x - y plane.)

The non-linear partial differential equation (18) with its boundary conditions is not easy to solve in full generality. Here we will consider only the simplest situation in which θ may be treated as small so that we may linearize $\sin \theta \approx \theta$. Furthermore, we consider only the static case with θ independent of time. Then (18) has the solution

$$\theta(x, y) = \frac{1}{\pi v^2 c e} I \sum_{m,n=-\infty}^{+\infty} f(x - \frac{L}{2} - nL, y - mW), \quad f(x, y) \equiv K_0(r/l) \quad (20)$$

where we have defined the characteristic length scale

$$l = \sqrt{cv^2/\eta} \quad (21)$$

determined by the capacitance per unit area, the velocity of propagation, and the tunneling amplitude. The overall constant I will be determined below. Recall the integral representation for the Bessel function

$$K_0(z) = \int_0^\infty dt e^{-z \cosh t} \quad (22)$$

and thus $K_0(x)$ and $K_0'(x)$ are respectively everywhere positive and everywhere negative for x real. The tunneling current $j_t = \eta \sin \theta \approx \eta \theta$ is everywhere positive (for I positive for definiteness) as we might have expected physically. For L and W large compared to other relevant distance scales, θ is dominated by two terms in (20) and thus we have the

flow pattern

$$j_{-,x} = \frac{1}{\pi l} \frac{I}{e} K'_0\left(\left[\left(x - \frac{L}{2}\right)^2 + y^2\right]^{\frac{1}{2}}/l\right) \frac{x - \frac{L}{2}}{\sqrt{\left(x - \frac{L}{2}\right)^2 + y^2}} + (L \rightarrow -L) + \dots \quad (23)$$

and

$$j_{-,y} = \frac{1}{\pi l} \frac{I}{e} K'_0\left(\left[\left(x - \frac{L}{2}\right)^2 + y^2\right]^{\frac{1}{2}}/l\right) \frac{y}{\sqrt{\left(x - \frac{L}{2}\right)^2 + y^2}} + (L \rightarrow -L) + \dots \quad (24)$$

We see that the current j_x is positive for $x \lesssim L/2$ while j_x is negative for $x \gtrsim -L/2$: the flow is towards the edge, in other words. For y positive, j_y is negative, while for y negative, j_y is positive: the flow is towards the x axis.

The overall coefficient I is fixed by the boundary condition (19) using the fact that $K_0(x) \rightarrow -\log x$ as $x \rightarrow 0$. Thus, near the two leads the current flows radially into the leads with magnitude $j_{-,r} = \frac{1}{\pi e} \frac{I}{r}$. Since $\vec{j}_- = \vec{j}_1 - \vec{j}_2$, at the lead on layer 1 electrons flow out of the system while at the lead on layer 2 electrons flow into the system. The net current flowing through the system is I . Matching the boundary condition we find

$$I = \frac{V_{ex} - V_{AB}}{R_{ex}} \quad (25)$$

In the static case, the voltage difference between the two layers vanishes but the voltage may depend on the position in the plane. Thus the voltage difference between the two contacts V_{AB} is not zero. In fact V_{AB} is equal to the Hall voltage in the two-terminal measurement of quantum Hall samples: $V_{AB} = \rho_{xy} I$ where $\rho_{xy} = mh/e^2$ for the (mmm) state. Therefore

$$I = \frac{V_{ex}}{R_{ex} + \rho_{xy}} \quad (26)$$

which is (17) with $R_{ex} \rightarrow R_{ex} + \rho_{xy}$. The relation (26) leads to a I - V_{ex} curve described in Fig. 2b. Note I/V_{ex} is finite even when $R_{ex} = 0$.

The critical current is no longer $A\eta$. It may be estimated as follows. The maximum value of θ occurs around the leads:

$$\theta_{max} \sim \frac{1}{4\pi v^2 c} \frac{I}{e} \ln(l/l_0) \quad (27)$$

where l_0 is a short distance cut-off length which depends on the details (such as the size) of the contact of the leads. The ‘‘average value’’ of θ is roughly

$$\theta_{average} \sim \frac{I}{eA\eta} = \frac{1}{4\pi v^2 c} \frac{I}{e} \left(\frac{4\pi l^2}{A} \right) \quad (28)$$

For our linear approximation to hold, the larger of these two values of θ must be less than $O(1)$. Two limits may be considered.

In the first limit, $A \gtrsim l^2$ (more precisely $A \gtrsim \frac{4\pi l^2}{\ln(l/l_0)}$), we find

$$I_c \sim \frac{4\pi e v^2 c}{\ln(l/l_0)} \frac{\hbar}{e^2} \quad (29)$$

which is not proportional to the area of the sample. (We have included the proper powers of e and \hbar .) The interlayer capacitance per unit area is given by $c = \epsilon/4\pi d$ where d is of order of the interlayer separation and ϵ the effective dielectric constant. Writing $v = f_v e^2 / \epsilon \hbar$, we find

$$I_c \sim \left(\frac{f_v^2}{\epsilon} \right) \frac{1}{\ln(l/l_0)} \frac{e^2}{d \hbar} e = \left(\frac{f_v^2}{\epsilon} \right) \frac{1}{\ln(l/l_0)} \frac{100 \text{\AA}}{d} 35 \mu\text{A} \quad (30)$$

Yang et al¹⁰ estimated the dimensionless coefficient f_v to be

$$f_v^2 \approx \frac{1}{4} \frac{d}{l_B} \int_0^\infty dx x^2 \exp\left(-\frac{x^2}{2} - x \frac{d}{l_B}\right) \quad (31)$$

. It depends on d/l_B and approaches zero when $d \rightarrow 0$. We have $f_v = 0.28$ for $d/l_B = 1$ and $f_v = 0.19$ $d/l_B = 3$. The dielectric constant $\epsilon \sim 10$. Thus very roughly $I_c \sim 10 - 100 \text{nA}$.

In the opposite limit $A \ll l^2$, θ is almost a constant and $I_c \sim A\eta < \frac{4\pi e v^2 c}{\ln(l/l_0)} \frac{\hbar}{e^2}$, just as in section II.

A striking feature of these results is that for the (mmm) state the two-terminal resistance between the two layers is either zero or $\rho_{xy} = mh/e^2$ depending on lead geometry regardless of how weak is the interlayer tunneling as long as the current is less than a critical value (whose magnitude is proportional to the interlayer tunneling strength in the weak tunneling limit).

Another point we would like to emphasize is that our results naturally cross over to the strong tunneling limit, in which case the (mmm) state becomes effectively a single layered $\nu = 1/m$ quantum Hall state. The two terminal resistance is given by $\rho_{xy} = mh/e^2$ as one would expect. This interpolating behavior gives us additional confidence in the reasonableness of our result.

IV. NARROW BAND NOISE AND AC EFFECTS IN INTERLAYER TUNNELING

In this section we are going to study dynamical AC effects in interlayer tunneling. We again consider a sample with a lead geometry in Fig. 3. When $V_{ex}/(R_{ex} + \rho_{xy}) > I_c$ the equation (18) can no longer support a static solution. To understand the time dependent solutions, we will for the sake of simplicity assume the velocity of the collective mode to be large, so that one can ignore the time delay for an electron to propagate from one lead to the other. In other words, we assume that the size of the region over which θ is coherent is larger than the sample size. In this case the voltage between the two layers is constant in space (although it may depend on time). Under this approximation θ has the form

$$\theta = \theta_0(t) + \delta\theta(x) \quad (32)$$

where $\delta\theta$ is independent of time and θ_0 is independent of space. The voltage V_{AB} in (19) is now given by

$$V_{AB} = I\rho_{xy} + \frac{\hbar}{e} \frac{d\theta_0}{dt} = \frac{V_{ex} - V_{AB}}{R_{ex}} \rho_{xy} + \frac{\hbar}{e} \frac{d\theta_0}{dt} \quad (33)$$

To obtain the time dependent tunneling current we need to solve (18) and (19). Integrating the two sides of (18) over the whole sample and using (32), we find

$$\begin{aligned} Ac \frac{d^2\theta_0}{dt^2} &= -\eta \int d^2x \sin(\delta\theta + \theta_0) + (R_{ex} + \rho_{xy})^{-1} (eV_{ex} - \hbar \frac{d\theta_0}{dt}) - R_{leak}^{-1} \hbar \frac{d\theta_0}{dt} \\ &= -A\tilde{\eta} \sin(\theta_0 + \alpha) + (R_{ex} + \rho_{xy})^{-1} (eV_{ex} - \hbar \frac{d\theta_0}{dt}) - R_{leak}^{-1} \hbar \frac{d\theta_0}{dt} \end{aligned} \quad (34)$$

where α is an irrelevant time independent constant. The effective tunneling amplitude has been reduced from η to $\tilde{\eta}$. This equation was studied in Ref. 2. We found that when $V_{ex}/(R_{ex} + \rho_{xy}) \gg A\tilde{\eta}$ we may treat the quantum tunneling term as a perturbation. The tunneling current $I = (R_{ex} + \rho_{xy})^{-1}(eV_{ex} - \hbar\frac{d\theta_0}{dt})$ is given by

$$\begin{aligned}
V &\approx V_* + \frac{I_c/((R_{ex} + \rho_{xy})^{-1} + R_{leak}^{-1})}{\sqrt{\left(\frac{V_*C}{(R_{ex} + \rho_{xy})^{-1} + R_{leak}^{-1}}\right)^2 + \frac{1}{4}}} \sin\left(\frac{eV_*}{\hbar}t\right) \\
&= V_* + \frac{2\Delta^2}{\sqrt{V_*^2 + \left(\frac{(R_{ex} + \rho_{xy})^{-1} + R_{leak}^{-1}}{2C}\right)^2}} \sin\left(\frac{eV_*}{\hbar}t\right) \\
I &\approx \frac{V_{ex}}{R_{ex} + \rho_{xy} + R_{leak}} + \frac{I_c}{\sqrt{((R_{ex} + \rho_{xy})CV_*)^2 + (1 + R_{leak}^{-1}(R_{ex} + \rho_{xy}))^2}} \sin\left(\frac{eV_*}{\hbar}t\right) \\
V_* &\equiv \frac{R_{leak}}{R_{ex} + \rho_{xy} + R_{leak}} V_{ex}
\end{aligned} \tag{35}$$

where $\Delta = \sqrt{\eta/c}$ is the gap of the neutral superfluid mode due to interlayer tunneling. The results in (35) is valid when the AC component in V is much less than the DC part V_* , that is when $V_{ex}/(R_{ex} + \rho_{xy}) \gg I_c$ or $V_*/\Delta \gg 1$. The DC current is given by $I_{DC} = V_{ex}/(R_{ex} + \rho_{xy} + R_{leak})$. Combining with the results from the last section, we find the I-V characteristics of the interlayer tunneling to have a behavior as presented in Fig. 2b.

From (35) we see that, in addition to a DC current, a large V_{ex} also induces an alternating current with frequency

$$\omega_* = \frac{R_{leak}}{R_{ex} + \rho_{xy} + R_{leak}} \frac{eV_{ex}}{\hbar} \tag{36}$$

Such an alternating current represents a narrow band noise with a δ -function spectral peak at ω_* . Here we would like to stress that the above result is obtained within a semiclassical approximation in which we treat θ as a classical field. In section 8, we will see that, under certain conditions, quantum corrections may generate a finite width in the spectral peak

of the narrow band noise. The width of the peak can be much less than Δ the energy gap of the neutral collective mode induced by interlayer tunneling. (See section 8).

V. GEOMETRY OF INTERLAYER COUPLING – POINT CONTACT AND SURFACE CONTACT

In Ref. 2, we derived the effective Lagrangian

$$L = \frac{1}{2}C(\partial_t\theta)^2 + \zeta \cos \theta \quad (37)$$

to describe tunneling in double layered Hall system, where $\zeta = A\eta$ for area coupling. (This is just (3) integrated over the area of the system, for space independent θ). Expanding the cosine term we see that the θ field has a mass or gap Δ proportional to $\sqrt{\frac{\zeta}{C}}$. The cosine term in (37) manifestly breaks the U(1) symmetry $\theta \rightarrow \theta + \text{constant}$. This is similar to the standard Landau-Ginzburg Lagrangian given in textbooks to describe Josephson tunneling between superconductors:

$$L = \frac{1}{2}C(\partial_t\theta_1)^2 + \frac{1}{2}C(\partial_t\theta_2)^2 + \zeta \cos(\theta_1 - \theta_2) \quad (38)$$

Simple geometrical considerations, however, indicate an important distinction between the two situations. In the usual discussion of Josephson junction, we have two bulk superconductors with an area contact, or even possibly a point contact, between them. In other words, the phenomenological coefficients C and ζ scales differently: C scales with the volume while ζ scales with the area. The gap scales to zero. Thus, in the thermodynamic limit the cosine term has vanishing effect on the dynamics of the θ field, which remains massless or gapless. In contrast, in the double layered Hall system, the geometry is such that C and ζ both scale like the area of the Hall fluid, and thus θ has a gap.

From this discussion, we see that, in order to have a close analog of the tunneling between two bulk superconductors, we should couple the two layers through only a single point. Such a point contact does not induce any gap in the collective mode (in the thermodynamic limit). In this case, the interlayer tunneling is similar to the Josephson tunneling between two bulk superconductors. A finite voltage between two layers should induce a narrow band noise in the tunneling current with a δ -function peak at frequency ω . We also expect that a small interlayer tunneling current will not induce any voltage drop across the point contact, which leads to the I-V characteristics displayed in Fig. 2.

For surface contact or finite sample, interlayer tunneling induces a gap in the collective mode. As we emphasized in Ref. 1, the current-current correlation function contain a pole at this gap Δ . One may think at first sight that the appearance of the gap would destroy the supercurrent (which requires the current correlation to have a pole at zero frequency.¹¹) Note however that the appearance of the gap is a non-perturbative effect in the expansion of the tunneling amplitude and that this gap would appear not only in the double-layered system, but also in ordinary coupled superconductors. When two three dimensional superconductors are coupled through a surface contact, the gap scales like $L^{-1/2}$, where L is the linear size of the system. For large systems the gap is small, and can be ignored. From this point of view, we see that a sufficient condition (which may not be necessary) to observe alternating tunneling current between two coupled superconductors or between the two layers of double layered Hall system is that $\Delta \sim \sqrt{\frac{\xi}{\mathcal{C}}}$ should be less than the frequency scale of interest (*e.g.*, the Josephson frequency). This consideration leads to a conservative estimate that the width of the narrow band noise should not exceed Δ .

A more delicate question is that whether we can observe a narrow band noise with a peak width much less than Δ ? The tunneling current in an open system (*i.e.*, double layered with leads) was discussed in the last section within the semiclassical approximation.

The noise spectrum was found to have a peak of zero width in the semiclassical approximation even for finite Δ . Although this result cannot be used to prove the true width of the peak to be exactly zero, it does suggest the possibility that the width of narrow band noise may be less than Δ . However, to gain a better understanding of the width of the noise peak, we need to understand the quantum corrections to the semiclassical calculation. Some discussion on the quantum corrections and their effects on the width of the narrow band noise can be found in section 8.

VI. RELATIONSHIP BETWEEN THE EASY PLANE FERROMAGNETS AND THE XY MODEL

Inspired by the earlier work of MacDonald and collaborators¹², Yang, Moon, Zheng, MacDonald, Girvin, Yoshioka, and Zhang⁵ have recently given an interesting description of the double layered quantum Hall system in terms of pseudospin or isospin. One associates with each electron an isospinor such if the isospin (to be referred to simply as spin henceforth) is up, the electron is in the upper layer, while if the spin is down, the electron is in the lower layer. In the hypothetical limit in which the interlayer and intralayer interactions are equal the system has an SU(2) invariance. A local magnetization density \vec{n} may be defined, obeying dynamics described by the energy functional $\lambda(\nabla n)^2 + V(n)$ with

$$V(n) = \frac{\beta}{2}n_z^2 - \eta n_x \quad (39)$$

Here $\beta = c^{-1}$ denotes the inverse "bare" capacitance and parametrizes the fact that the interlayer interaction is stronger than the intralayer interaction, and η is proportional to the tunneling amplitude. It is easy to see in this spin formalism the tunneling operator is given essentially by $2S_x = S_+ + S_-$ since the raising and lowering operators take an electron from one layer to the other.

Here we would like to discuss the relationship of this spin model with the Lagrangian (4) we used in Ref. 2. The Lagrangian description of spin systems has been discussed by numerous authors; here we follow the discussion given in Ref. 13 which we now review briefly. The Lagrangian is given by

$$L = -iz^\dagger \dot{z} - V(n) \quad (40)$$

For simplicity, we have dropped the spatial gradient term $(\nabla n)^2$ since we are only interested in the limit in which the wave vector $\vec{k} \rightarrow 0$ in this section. Here the spinor z is such that $\vec{n} = z^\dagger \vec{\sigma} z$. Using the identity $\delta(z^\dagger \dot{z}) = \text{constant} \delta \vec{n} (\vec{n} \times \dot{\vec{n}})$ we obtain the equation of motion

$$\vec{n} \times \dot{\vec{n}} = \frac{\delta V}{\delta \vec{n}} \quad (41)$$

Taking the scalar product of this equation with \vec{n} we obtain

$$\dot{\vec{n}} = \vec{n} \times \frac{\delta V}{\delta \vec{n}} \quad (42)$$

In the usual spherical coordinates for the unit vector \vec{n} the spinor z is given by

$$z = \frac{1}{\sqrt{2}} (\cos(\theta/2) e^{i\varphi/2}, \quad \sin(\theta/2) e^{-i\varphi/2}) e^{i\alpha} \quad (43)$$

The phase angle α decouples from the system and may be dropped. Inserting this into (40) we find (after dropping an irrelevant factor of 1/8) that

$$L(\theta, \varphi) = \hbar \cos \theta \dot{\varphi} - \frac{\beta}{2} \cos^2 \theta + \eta \sin \theta \cos \varphi \quad (44)$$

where we have reinstated Planck's constant \hbar .

Conceptually, there is now no difficulty in reducing this Lagrangian to an effective Lagrangian. We wish to integrate the "high energy" field θ in the path integral

$$\int D \cos \theta e^{\frac{i}{\hbar} \int dt L(\theta, \varphi)} = e^{\frac{i}{\hbar} \int dt L_{eff}(\varphi)} \quad (45)$$

where the effective Lagrangian will have the form

$$L_{eff}(\varphi) = A(\varphi) + B(\varphi)\dot{\varphi}^2 + \dots \quad (46)$$

By a symmetry argument, it is easy to see that only terms with even powers of time derivatives are generated. Unfortunately we are not able to evaluate this integral exactly and we have to resort to various limits. It is perhaps clearer to deal with the equations of motion directly. In the limit $\beta \gg 1$, the vector \vec{n} is forced to lie mostly in the $x - y$ plane. We are interested in the dynamics of its orientation in this plane. (Note incidentally that in this section we adhere to the standard notation for spherical coordinates in which the azimuthal angle is denoted by φ . Unfortunately, the field variable in the sine Gordon theory is denoted by θ in the literature and in our previous work. It is the azimuthal angle φ of this section which corresponds to the field θ in the other sections in this paper.)

The Euler-Lagrange equations of motion are

$$\dot{\theta} = \eta \sin \varphi \quad (47)$$

and

$$\dot{\varphi} = \beta \cos \theta + \eta \text{ctg} \theta \cos \varphi \quad (48)$$

For $\beta \gg 1$, the angle θ is close to $\pi/2$. We linearize (48) in $\theta - \pi/2$ and substitute in (47) to obtain

$$\ddot{\varphi} + \frac{\eta}{(\beta + \eta \cos \varphi)} \sin \varphi \dot{\varphi}^2 = -(\beta + \eta \cos \varphi) \eta \sin \varphi \quad (49)$$

If we now impose further the condition $\beta \gg \eta$ then we obtain

$$\ddot{\varphi} = -\beta \eta \sin \varphi \quad (50)$$

We thus obtain the sine Gordon theory discussed in (4) and (37) in previous sections.

As was emphasized in Ref. 2 and section II, we derive the effective Lagrangian (4) by the following procedure. We start with an effective Chern Simons theory, which is

guaranteed by general principles to be valid at low frequencies and wave vectors. We then go through an instanton (monopole) calculation valid in the dilute gas approximation, corresponding to the limit in which the tunneling amplitude is small, and obtain the sine Gordon theory description of tunneling through double layered Hall systems. Thus, in the limit of low frequencies and wave vectors, and in the limit of small tunneling amplitude (so that the resulting gap is small and hence the relevant frequencies are small), any theory describing the double layered Hall system must reduce to the sine Gordon theory. In this section we have verified that this is indeed the case.

On the other hand, the theory described in (44) and the sine Gordon theory clearly should not be compared in the limit in which the tunneling parameter η is not small compared to β . For instance, expanding (49) for small φ one finds immediately that the frequency of oscillation is given by

$$\omega^2 = (\beta + \eta)\eta \quad (51)$$

as was derived by Yang et al.⁵ It was remarked that as β goes to zero, the gap remains finite. In contrast, the gap given by the sine Gordon theory (50) is equal to $\beta\eta$ which vanishes as β goes to zero, but this is in a regime where the sine Gordon theory is not valid!

We note in passing that (49) follows from the effective Lagrangian

$$L = \frac{\beta}{(\beta + \eta \cos \varphi)^2} \frac{\dot{\varphi}^2}{2} + \log\left(\frac{\beta + \eta \cos \varphi}{\beta}\right) \quad (52)$$

This effective Lagrangian may be valid beyond the regime $\eta \ll \beta$.

Let us now impose a voltage across the double layered system by adding to $V(n)$ in (39) a term Un_z which says that for an electron to have its isospin up costs more energy than to have its isospin down. It is tempting to equate the parameter U with the voltage. However, as emphasized in Ref. 2 the voltage is correctly defined as the energy it costs

to move an electron from the lower layer to the upper layer, and this is not equal to U . (In the notation of Ref. 2 U corresponds to U_0 .) Another point worth emphasizing is that the voltage across the two layers is, strictly speaking, defined only when the tunneling amplitude is small. When the tunneling amplitude is large, the system effectively behaves like a single layer and the concept of voltage is ill defined. Thus, strictly speaking, we should not work with the spin Hamiltonian but pass directly to the sine Gordon theory. From (44) for example we see that adding the term Un_z has the effect of shifting $\dot{\varphi}$ to $\dot{\varphi}-U$. The effect of the voltage thus amounts to a shift in the sine Gordon theory as discussed in detail in Ref. 2. A simple calculation of the energy required to move an electron from one layer to another shows that the voltage V is given by

$$V = \dot{\varphi} \tag{53}$$

Our circuit equation (13) then follows.

VII. FOUR TERMINAL MEASUREMENT – EXPERIMENTAL TEST OF ZERO VOLTAGE DROP BETWEEN LAYERS

In this section we would like to consider how to experimentally test the prediction that a small interlayer tunneling current does not induce any voltage drop between the two layers for the (mmm) state. One way to test the zero voltage drop is through a sample with the geometry described in Fig. 4. The M region is occupied by the (mmm) state and R and L region by a metallic state (*e.g.*, the $\nu = 1/2$ state) in the first and second layer respectively. The metallic state in the R and L region serve as ohmic contacts to the first and second layer in the (mmm) state. One voltage probe is attached to an edge of the (mmm) state in the first layer, and another attached to the edge on the same side in the second layer (see Fig. 4). As we pass a current from the R region to the L region, the

current must tunnel through the barrier between the two layer. According to Ref. 2 the voltage drop between the two voltage probes should be zero if the current is less than a critical value, as represented in Fig. 2a. Again the striking feature is that the voltage drop is zero even for weak interlayer tunneling. Weak interlayer tunneling only leads to a small critical current.

We would like to make three remarks.

- 1) If the second probe is attached to the edge on the other side of the sample, a non-zero voltage drop will appear due to the non-zero Hall resistance.
- 2) The vanishing of the voltage drop between the two leads is a consequence of the superfluid mode, not of the chirality of the edge excitations (*i.e.*, the absence of back propagating modes). To illustrate this point let us replace the (mmm) state in the M region by a $(mm0)$ state, which does not have any superfluid mode (*i.e.*, its K -matrix does not have a zero eigenvalue). There is no quantum coherence between the two separate $1/m$ states in the two layers. Now interlayer tunneling is controlled by tunneling between the two edges of the two $1/m$ states. In this case a finite current will produce a finite voltage drop between the two layers and hence between the two voltage probes. If the edges are sharp on the scale of the magnetic length, we have¹⁴ $V \propto I^{1/(2m-1)}$ at zero temperature $T = 0$ and $(\frac{dI}{dV})_{V=0} \propto T^{2m-2}$.
- 3) In the strong tunneling limit, the (mmm) state crosses over to a single layered $\nu = 1/m$ state. The zero voltage drop between the two leads is just the standard result $\rho_{xx} = 0$ for FQH states. This correct cross-over behavior from the weak to the strong tunneling limit further confirms the validity of our results.

VIII. SEMICLASSICAL APPROXIMATION

The result of vanishing voltage for small interlayer tunneling currents and the appearance of narrow band noises are supported by two calculations which involve different approximations. In this section we will discuss the semiclassical approximation; in the next section we will present a perturbative calculation.

In Ref. 2 we used the semiclassical approach in which one ignores quantum fluctuations and treats θ as a classical field. We calculated the interlayer tunneling current by solving the classical equation of motion for θ , as we did to obtain (34). The textbook justification for the semiclassical approach, commonly used to study the tunneling between superconductors, is based on the fact that θ is conjugate to $N_- = N_1 - N_2$, the difference in electrons (or Cooper pairs) between the two layers, and thus the quantum uncertainty $\Delta\theta \sim 1/\Delta N_-$ may be made very small while keeping $\Delta N_-/N_- \ll 1$.

In this section we will examine the validity of the semiclassical approach in the simplest case of an isolated double-layered system. Let us consider the limit in which v/L is larger than any energy scales of interest (*e.g.*, $v/L > \Delta$), where L is the linear size of the system. In this limit we can take θ to be constant in space. The Lagrangian of the system becomes

$$L = \frac{C}{2}(\dot{\theta})^2 + \zeta \cos \theta \quad (54)$$

The above Lagrangian describes a mass C particle moving on a circle parametrized by θ . In the classical limit, both the position and the velocity of the particle are well defined. The motion of the particle (with energy higher than the potential barrier) in a periodic potential induces a periodic tunneling current $I \propto \sin \theta$. To understand the quantum corrections, let us construct a moving wave packet

$$\psi(\theta) = e^{-\theta^2/2\xi^2} e^{ik\theta} \quad (55)$$

The average velocity of the wave packet is $v_p = k/C$. The spread of the wave packet produces the quantum corrections to the above classical picture.

The uncertainty in the velocity of the wave packet receives two contributions. One is from the uncertainty of the momentum, $\frac{1}{C\xi}$, and the other from the uncertainty of the potential energy within the wave packet, $\frac{\zeta\xi}{k}$. Both contributions are due to the finite size of the wave packet. The total uncertainty in the velocity can be estimated as

$$\Delta v_p \sim \frac{1}{C\xi} + \frac{\zeta\xi}{k} \quad (56)$$

Thus at time t the width of the wave packet is

$$\Delta\theta = \xi + \Delta v_p t \sim \left(\frac{\zeta t}{k} + 1\right)\xi + \frac{t}{C} \frac{1}{\xi} \quad (57)$$

The minimum width can be obtained by varying ξ , and we find

$$\Delta\theta \sim \sqrt{\left(\frac{\zeta t}{Cv_p} + 1\right) \frac{t}{C}} \quad (58)$$

At time

$$t_0 = \frac{\sqrt{v_p^2 + 4\zeta v_p} - v_p}{2\zeta} C \quad (59)$$

$\Delta\theta$ becomes of order 1. We know that the motion of the wave packet cause an alternating tunneling current of frequency $\omega = v_p$. $1/t_0$ can be thought as the decay rate of the alternating current due to the quantum correction. Thus the motion of the wave packet give rise to a narrow band noise at frequency ω with a band width

$$\begin{aligned} \Delta\omega &\sim \frac{1}{t_0} \\ &= \frac{e^2}{\hbar C} \frac{2\frac{I_c}{e}}{\sqrt{\omega^2 + 4\frac{I_c}{e}\omega - \omega}} \\ &= \frac{e^2}{\hbar C} \quad \text{when } \frac{I_c}{e} \ll \omega \end{aligned} \quad (60)$$

where we have restored \hbar and e . We see that in the weak tunneling limit or when the voltage between the two layers is not too small, the band width of the narrow band noise

is of order of the charging energy between the two layers, which can be much less than the gap $\Delta = (\zeta/C)^{\frac{1}{2}}$ of the neutral collective mode. We also notice that $\Delta\omega/\omega$ approaches 1 when

$$\omega = \frac{eV}{\hbar} \rightarrow \left(\frac{e^4}{\hbar^2 C^2} \frac{I_c}{e}\right)^{1/3} \quad (61)$$

if $(\frac{e^4}{\hbar^2 C^2} \frac{I_c}{e})^{1/3} < \frac{I_c}{e}$. We find that well defined narrow band noise exists (*i.e.*, $\Delta\omega < \omega$) when, at least, the following conditions are satisfied:

$$\max\left(e^2/\hbar C, [(e^4/\hbar^2 C^2)(I_c/e)]^{1/3}\right) < \omega = eV/\hbar < v/L \quad (62)$$

To confirm the above rough estimates, we have done some numerical calculations to determine the time evolution of the wave packet in (55) using the following Hamiltonian

$$H = -\frac{e^2}{2C} \frac{d^2}{d\theta^2} - \zeta \cos \theta \quad (63)$$

For $\zeta/(e^2/C) = 150$, the frequency spectrum of the tunneling current $I = e\zeta\langle\sin\theta\rangle$ is plotted in Fig. 5 for $k = 100$ and $k = 40$, where the frequency ω is measured in unit of the charging energy e^2/C . From the numerical results we see that

- 1) The noise spectrum contain many peaks. The peaks occur at roughly the Josephson frequency $\omega_J = \langle\dot{\theta}\rangle \approx ke^2/C$. The separation between the peaks is very close to e^2/C . The width of each peak is much less than the charging energy e^2/C . In our numerical result the width is limited by the numerical resolution.
- 2) The width of the cluster of the peaks is of order $5e^2/C$, which is less than the gap for the neutral mode $\Delta = 12e^2/C$. The width that we estimated above (Eq. (60)) agrees well with the width of the cluster.

For a typical double layer sample of size $10\mu \times 10\mu$, the charging energy is of order 60MHz. However the energy scale associated with interlayer tunneling $\zeta = I_c/e \sim N\Delta_{SAS}$ is very very large (here N is the number of electrons in each layer). One needs to fine tune the transverse magnetic field to make ζ almost zero in order to satisfy the condition (62).

We would like to stress that the above result of finite band width of the narrow band noise in tunneling current is not a particular property of tunneling in the double layered systems. The same result also applies to the Josephson tunneling between superconductors, once we replace e in (60) by $2e$. In this case C still represents the capacitance of the junction and ω represents the Josephson frequency. It would be very interesting to see whether one can observe the quantum correction to the Josephson effects in tunneling between small superconductors.

We also would like to stress that the discussion in this section does not include the effects of dissipation coming from the contact to the leads. The shape of the noise spectrum may be changed by the dissipation effects. Also the condition to observe the narrow band noise (62) may be relaxed in presence of leads.

IX. PERTURBATIVE CALCULATION AND INTERLAYER TRANSPORT AT FINITE TEMPERATURES

In this section we are going to study the properties of interlayer tunneling using a perturbative expansion of the tunneling amplitude. In particular we would like to study the noise spectrum and I-V characteristics at finite temperatures (within the perturbation theory). The calculation can be done for local coupling and for random coupling. We find that the tunneling current is given by $I \propto V^\gamma$ at finite temperatures. The temperature dependent exponent satisfies $\gamma \rightarrow 0$ as $T \rightarrow 0$ and $\gamma \rightarrow 1/4$ as T approaches the K-T transition temperature T_{KT} . The differential conductance at $V = 0$ is infinite. Again we see that the interlayer tunneling is drastically enhanced in the (mmm) state.

We know that the noise spectrum of the tunneling current is defined by

$$F(\omega) = \int_0^\infty dt \operatorname{Re}\langle j_T(t)j_T(0)\rangle e^{-i\omega t} \quad (64)$$

with j_T the interlayer tunneling current

$$j_t = i \int d^2x [t(x)c_1^\dagger(x)c_2(x) - h.c.]. \quad (65)$$

(where c_i represents an electron annihilation operator in layer i .)

At zero temperature, due to the long range order $\langle c_1^\dagger(x)c_2(x) \rangle \neq 0$, the noise spectrum $F(\omega)$ has an δ -function peak at eV/\hbar (within perturbation theory of tunneling t).² At finite temperatures (but below the Kosteritz-Thouless (KT) transition) the double layered system has an algebraically decaying order parameter just as in any 2D superfluids (*i.e.*, $\langle (c_1^\dagger c_2)_x (c_2^\dagger c_1)_0 \rangle \sim |x|^{-\gamma_{KT}}$). The dynamical correlation of $A \equiv c_2^\dagger c_1$ in imaginary time can be obtained from the Coulomb gas picture described in Ref. 2:

$$\langle A^\dagger(\tau, x)A(0) \rangle \propto \exp\left(\frac{e^2}{4\pi cv\sqrt{v^2\tau^2 + x^2}}\right) \quad (66)$$

where c is the capacitance per unit area between the two layers and v is the velocity of the gapless mode. At a finite temperature T and for real time we have (after an analytic continuation)

$$\langle \mathcal{T}(A^\dagger(t, x)A(0)) \rangle = \exp\left(\frac{e^2}{4\pi cv} \sum_n \frac{\sqrt{b_n + a_n}}{(2^{1/2}b_n)}\right) \exp\left(\text{sgn}(t) \frac{ie^2}{4\pi cv} \frac{\theta(v^2t^2 - x^2)}{\sqrt{v^2t^2 - x^2}}\right) \quad (67)$$

with

$$a_n = x^2 - v^2t^2 + n^2v^2T^{-2}, \quad b_n^2 = a_n^2 + 4v^4t^2n^2T^{-2} \quad (68)$$

For large x we find

$$\langle \mathcal{T}(A^\dagger(0, x)A(0)) \rangle \sim |x|^{-\gamma_{KT}} \quad (69)$$

with $\gamma_{KT} = \frac{Te^2}{2\pi cv^2}$ and for large t we have

$$\langle \mathcal{T}(A^\dagger(t, 0)A(0)) \rangle \sim |t|^{-\gamma_{KT}} \exp(is\text{gn}(t) \frac{e^2}{4\pi cv^2t}) \quad (70)$$

At finite voltage we should include a factor $e^{i\frac{eV}{\hbar}t}$ in the above result. Thus, at finite T , $F(\omega)$, determined by $\text{Re}\langle \mathcal{T}(A^\dagger(t, 0)A(0)) \rangle \sim t^{-\gamma_{KT}}$, has only an algebraic singularity at $\omega = eV/\hbar$, if the tunneling only occurs at isolated points (*i.e.*, $t(x) \propto \delta(x)$):

$$F(\omega) \sim \sin(\gamma_{KT})\Gamma(1 - \gamma_{KT}) \left|\frac{eV}{\hbar} - \omega\right|^{-\gamma_{KT}-1} \quad (71)$$

The DC tunneling I-V curve can also be calculated from the correlation of the tunneling current and is determined by $\text{Im}\langle\mathcal{T}(A^\dagger(t,0)A(0))\rangle \sim t^{-\gamma_{KT}-1}$. We found

$$I \propto \sin(\gamma_{KT})\Gamma(-\gamma_{KT})V^{\gamma_{KT}} \quad (72)$$

The temperature dependent exponent γ_{KT} is of order T/T_{KT} .¹⁵ At $T = T_{KT}$, γ_{KT} is equal to an universal value $1/4$ which is independent of m (Here we are considering interlayer tunneling in the (mmm) FQH state). The results (71) and (72) are also valid in the presence of impurities and of a magnetic field parallel to the plane. In that case $t(x)$ in (65) has a random phase and $\langle t(x) \rangle = 0$.

DISCUSSION

After completing the present paper, several experimental^{4,16} and theoretical papers^{17,18,19} appeared. The experiments in Ref. 4,16 show a dramatic enhancement in zero-bias conductance in interlayer tunneling. The measured zero-bias conductance is about $1/200\text{Kohm}$. Although the conductance is still smaller than the predicted value $1/25\text{Kohm}$, the measured conductance is getting smaller as one improve the quality of experiments. The experiments in Ref. 16 also observed the neutral superfluid mode and measure its velocity $v = 1.4 \times 10^4 m/s$. This velocity is about 3 to 5 times smaller than theoretical estimate.

Before applying our results to the real sample, we would like to point out that in our calculation we did not include effects of vortices in the phase field θ . Due to the random phase in the interlayer tunneling amplitude, the vortices may exist in the real sample. However, even in the presence of the vortices, our calculations are still valid *provided that the vortices are all pinned and do not move*. The pinned vortices just behave like random phase in the tunneling amplitude.

In the real sample used in Ref. 4,16, the interlayer separation is about $d \sim 2^{-6}cm$, the dielectric constant $\epsilon \sim 10$, the total electron density $n = 5 \times 10^{10}cm^{-2}$, and $\Delta_{SAS} = 90\mu K$. We find the characteristic length l is

$$l = \sqrt{\frac{\epsilon v^2 \hbar^2}{2\pi e^2 n \Delta_{SAS} d}} = 1\mu m$$

Since l is less than the size of the leads, we cannot treat the lead as a point contact. Since the interlayer tunneling current is non-zero only in a stripe of width l around the lead, we find the critical tunneling current to be

$$I_c \sim l w \eta = \frac{e l w n \Delta_{SAS}}{2\hbar} = 500 \frac{w}{1\mu m} pA$$

where w is the width of the lead. We note that the observed critical current $I_c \sim 15pA$ is much smaller. This could be due to the randomness in the phase of the interlayer tunneling amplitude and/or vortex motion which were ignored in the above discussion.

In the absence of interlayer tunneling, there is a KT transition in the double layered system. The transition temperature is

$$T_{KT} \sim \frac{v^2 \epsilon \hbar^2}{2e^2 d} = 170mK$$

We note that the enhancement of the zero bias conductance appears around $T = 170mK$. The gap of the neutral mode is

$$\Delta = \sqrt{\frac{2\pi n e^2 \Delta_{SAS} d}{\epsilon}} = 8\mu eV = 90mK$$

Since $\Delta < T_{KT}$, the system starts to show signs of superfluid properties. The superfluid properties will be more clear if $\Delta \ll T_{KT}$. For the present value of Δ_{SAS} , it may be hard to see a sharp KT transition. However, Δ_{SAS} can be reduced by a strong parallel magnetic field. The reduced Δ_{SAS} may make interlayer tunneling hard to observe. But one may be able to use capacitance coupling or surface phonon to probe the neutral superfluid mode which carries a dipole moment perpendicular to the layer.

For the present value of Δ_{SAS} and the sample size $L = 0.25mm$, we find (62) cannot be satisfied. Also since vortices may move near the critical current. Thus our discussion AC Josephson effect may not apply to the present sample. In order for our discussion to apply, one needs find ways to avoid vortex motion. One way to achieve that is to make l larger and to make sample smaller than l . Similarly Δ_{SAS} may still be too large for our perturbative calculation of the I-V curve at finite temperatures to be apply.

The recent theory papers ^{17,19} start with the effective theory (4) first proposed in Ref. 1,2 which pointed the spontaneous $U(1)$ symmetry breaking in the system without interlayer tunneling. The same effective theory also describe tunneling bwteen superconducting thin films. Thus those theoretical results also apply to tunneling bwteen superconducting thin films. The effects of vortex flow and other dissipations has been discussed by Stern, Girvin, MacDonald, and Ma¹⁷, and by Fogler and WilczekRef. 19. They find vortex flow can indeed reduce the zero bais conductance from the ideal value e^2/h . The finite temperature I-V curve was also obtained by Balents and Radzihovsky¹⁸ where more general situations were considered. In particular, we would like to point out that Fogler and Wilczek found a strong “AC Josephson effect” (defined as a peak at frequency eV/h in noise spectrum of the tunneling current) even in the presence of vortex flow. Observing such an “AC Josephson effect” at frequency eV/h instead of $2eV/h$ will show a fundamental distinction between the (111) double-layer system and coupled superconducting thin films.

ACKNOWLEDGMENTS

We thank M. P. A. Fisher, A. MacDonald, and S. C. Zhang for very helpful discussions. This research is supported in part by the National Science Foundation under Grants DMR-9022933 (XGW) and PHY89- 04035 (AZ).

REFERENCES

1. X.G. Wen and A. Zee, *Phys. Rev. Lett.* **69**, 1811 (1992).
2. X.G. Wen and A. Zee, *Phys. Rev.* **B47**, 2265 (1993).
3. H.A. Fertig, *Phys. Rev. B* **40**, 1087 (1989).
4. I. B. Spielman, J. P. Eisenstein, L. N. Pfeiffer, K. W. West, *Phys. Rev. Lett.* **84**, 5808 (2000).
5. K. Yang, K. Moon, L. Zheng, A. MacDonald, S. Girvin, D. Yoshioka, and S.-C. Zhang, *Phys. Rev. Lett.* **73**, 732 (1994)
6. A.H. MacDonald, P.M. Platzman, and G.S. Boebinger, *Phys. Rev. Lett.* **65**, 775 (1990). See also L. Brey, *ibid.* **65**, 903 (1990) and H. Fertig, *Phys. Rev. B* **40**, 1087 (1989).
7. X.G. Wen and A. Zee, *Phys. Rev.* **B46**, 2290 (1992).
8. X.G. Wen and A. Zee, *Nucl. Phys. (Suppl.)* **B15**, 135 (1990); B. Blok and X.G. Wen, *Phys. Rev.* **B42**, 8133 (1990); *Phys. Rev.* **B42**, 8145 (1990); N. Read, *Phys. Rev. Lett.* **65**, 1502 (1990); X.G. Wen and A. Zee, *Phys. Rev.* **B46**, 2290 (1992); J. Fröhlich and A. Zee, *Nucl. Phys.* **B364**, 517 (1991).
9. S.Q. Murphy, J. P. Eisenstein, and G. S. Boebinger, L. N. Pfeiffer and K. W. West, to be published.
10. The coefficient in front of $(\partial_i\theta)^2$ in (3) was given in Ref. 5, from which we can estimate the coefficient f_v .
11. A. H. MacDonald and Shou-Cheng Zhang, *Phys. Rev.* **B49**, 17208 (1994).
12. M. Rasolt and A.H. MacDonald, *Phys. Rev.* **34**, 5530 (1986).

13. X.G. Wen and A. Zee, *Phys. Rev. Lett.* **61**, 1025 (1988).
14. X.G. Wen, *Int. J. Mod. Phys.* **B6**, 1711 (1992).
15. Y.B. Kim, and X.G. Wen, *Phys. Rev.* **B48**, 6319 (1993).
16. I. B. Spielman, J. P. Eisenstein, L. N. Pfeiffer, K. W. West, cond-mat/0012094.
17. Ady Stern, S.M. Girvin, A.H. MacDonald, Ning Ma, *Phys. Rev. Lett.* **86**, 1829 (2001).
18. Leon Balents, Leo Radzihovsky, *Phys. Rev. Lett.* **86**, 1825 (2001).
19. Michael M. Fogler, Frank Wilczek, *Phys. Rev. Lett.* **86**, 1833 (2001).

FIGURE CAPTIONS

Fig. 1 Effective circuit diagram of the interlayer tunneling.

Fig. 2 DC I-V characteristics of the interlayer tunneling. Different I-V curves correspond to different lead geometries.

Fig. 3 A rectangular double layered system with point-like leads.

Fig. 4 Lead configuration for a four terminal measurement.

Fig. 5 Noise spectrum for interlayer tunneling current.

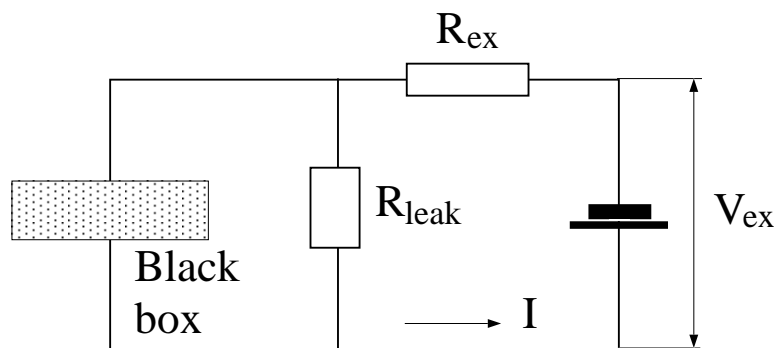


Fig. 1

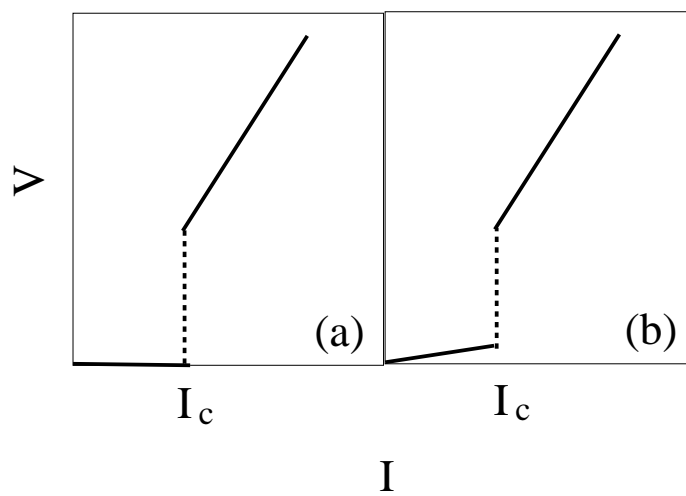


Fig. 2

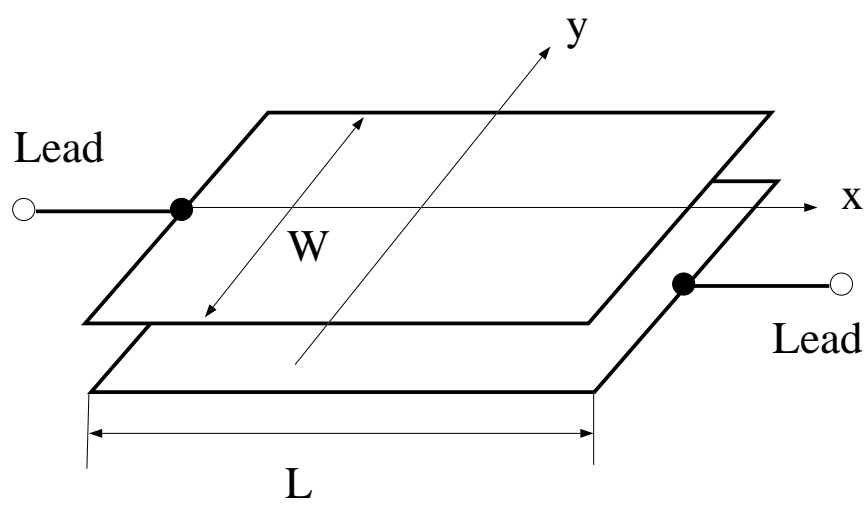


Fig. 3

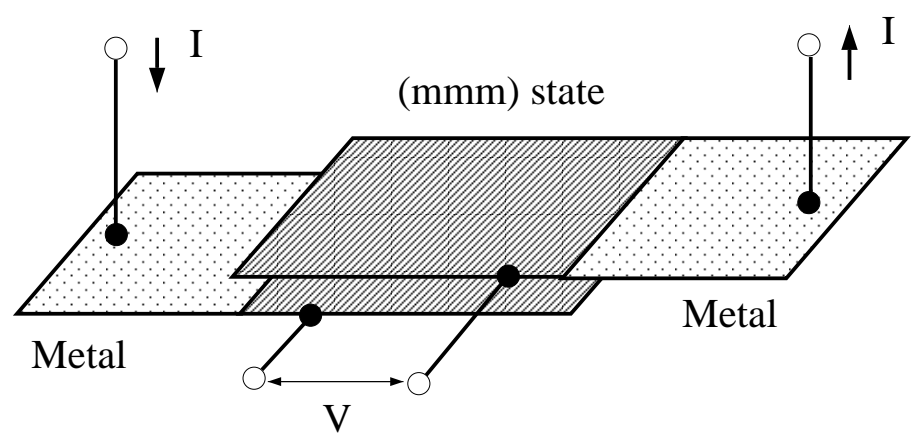


Fig. 4

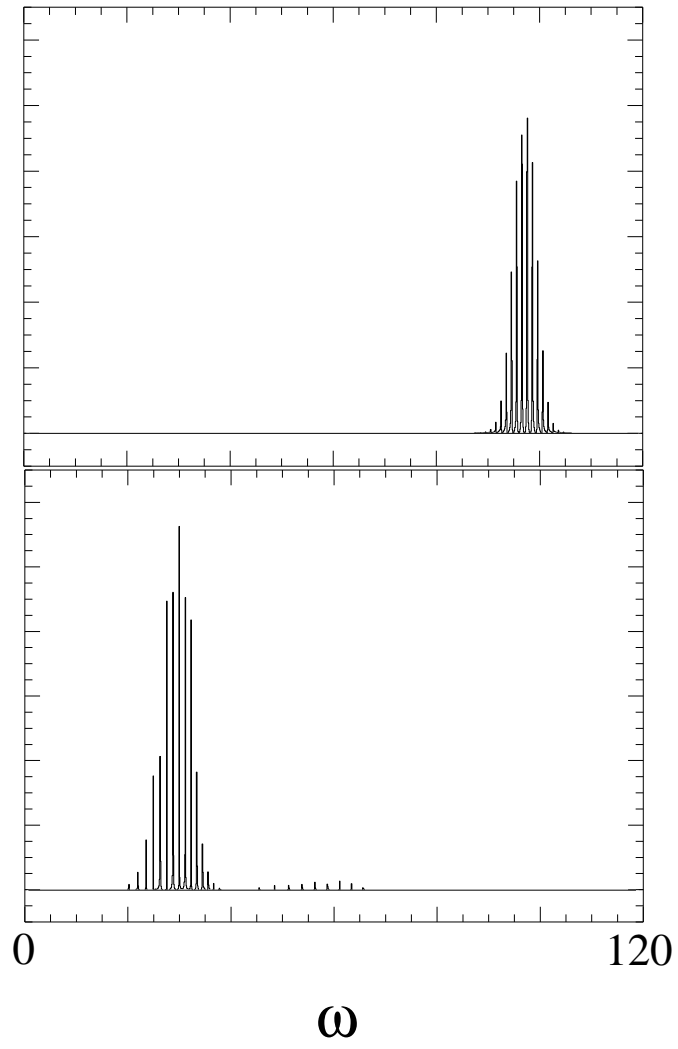


Fig. 5